ELSEVIER

Journal of Power Sources 97–98 (2001) 232–234

JOURNAL OF POWER SOURCES

www.elsevier.com/locate/jpowsour

Antimony doping effect on the electrochemical behavior of SnO_2 thin film electrodes

J. Santos-Peña[a], T. Brousse[a], L. Sánchez[b], J. Morales[b], D.M. Schleich[a,*]

[a]*Laboratoire de Génie des Matériaux, Ecole Polytechnique de l'Université de Nantes, rue Christian Pauc BP 90604, F44306 Nantes Cedex 3, France*

[b]*Laboratorio de Química Inorgánica, Campus Rabanales, Edif. C3, E-14071 Córdoba, Spain*

Received 16 June 2000; accepted 31 December 2000

Abstract

Tin dioxide- and antimony-doped tin dioxide thin films were prepared by using a sol–gel technique. Films are homogeneous in composition and morphology and show a remarkable decrease in the grain size (a few nanometers) and resistivity with doped antimony. Films were tested as potential anodes in lithium-ion batteries. The best electrochemical performance was obtained from the Li/''5% Sb''SnO_2, which provides more than 250 mAh/g during 75 cycles, meanwhile the Li/SnO_2 cell capacity fades after a few cycles. Good electrochemical behavior of the doped systems by rapport to the non-doped ones are discussed in terms of their mechanical and electronic properties.

Keywords: Lithium-ion batteries; Doped tin oxide; Thin films

1. Introduction

Since the announcement by Fuji Film Co., on the use of tin oxides as anodes for lithium-ion batteries, there has been an impressive amount of work on tin-based electrodes [1]. One of the problems related to the use of tin dioxide is that very fine particles are needed to get the high capacity expected for this material. Furthermore, the poor electronic conductivity of SnO_2 also hinders the reaction with lithium during the first discharge. In order to investigate the effect of the grain size and the electronic conductivity of tin dioxide, we have prepared thin films of this material by a sol–gel technique. The electronic conductivity was enhanced by antimony doping [2]. Furthermore, it seems that some dopants, like Mo, enhance the cycling properties of SnO_2 [3].

2. Experimental

Thin films were prepared from 1,3 propanediol solutions with a total metal concentration [Sn + Sb] equal to 0.05 M. These solutions were obtained from chlorides ($SnCl_4$, $SbCl_5$). $AgNO_3$ titration was used in order to remove chlorine ions which can introduce a random n-type doping in the films. About 7–10 ml of the solution was slowly sprayed on a 0.05 mm thick Stainless Steel foil (Goodfellow) at 498 K. Then, the films were annealed at 673 K for 1 h. These electrodes were examined by scanning electron microscopy (SEM) with a Leica stereoscan 440 instrument. XRD measurements were carried out on a Philips PW1710 diffractometer, using Cu Kα radiation. Electrochemical tests were performed at 25°C, in a simple two electrode cell using metallic lithium as both reference and counter electrode. The electrolyte was a 1 M solution of $LiPF_6$ dissolved in a 2:1 mixture of EC and DEC (Merck).

3. Results and discussion

Thin films obtained by this sol–gel technique have different colors, from white (0% Sb) to grey (10% Sb), depending on the antimony doping level. Scanning electronic microscopy was used to examine films morphology and thickness. No special change in electronic morphology occurs with antimony doping. Films thickness are in the order of a few microns. In addition, EDX analysis coupled with the microscope reveals that there is no antimony oxide particles apart from tin–antimony oxide particles. EDX

* Corresponding author. Tel.: +33-240-683127; fax: +33-240-683199.
E-mail address: donald@isirec4.isitem.univ-nantes.fr (D.M. Schleich).

0378-7753/01/$ – see front matter
PII: S0378-7753(01)00620-6

Table 1
Structural data of the antimony-doped tin oxide samples

Theoric % Sb	EDX % Sb	Proposed formula[a]	Particle microsize (nm)	a_0 (Å)	c_0 (Å)	Slice resistivity (Ω cm)	Sheet resistivity (kΩ cm^2)
0	0	SnO_2	5.1	4.74(3)	3.18(9)	>100	>100
5	5	$Sb_{0.05}Sn_{0.94}[\ ]_{0.01}O_2$	3.3	4.74(7)	3.18(6)	1.32	3.60
10	12	$Sb_{0.10}Sn_{0.87}[\ ]_{0.03}O_2$	2.9	4.73(5)	3.19(8)	2.15	5.40

[a] Empty sites are indicated by square brackets.

analysis were also used to quantify the antimony content of the samples (see Table 1). Since tin and antimony have very close Lα radiation we must be careful taking this data into account. Nevertheless, the observed contents agree quite well with the expected ones. X-ray diffraction (XRD) patterns (Fig. 1a and b) reveal a poor crystallinity of the samples according to the marked broadness of the peaks. Nevertheless, the peaks can be easily correlated to a cassiterite (SnO_2) structure, meanwhile other possible phases, such as antimony oxides (Sb_2O_x, $x = 3, 4, 5$), are not observed. Average values found for the crystallite size by using the Scherrer equation are collected in Table 1. Antimony doping remarkably decreases the crystallite size of the samples. In fact, crystallite sizes are 36 and 44% smaller for the 5% Sb and the 10% Sb samples, respectively, to those observed for non-doped tin oxide. This behavior has been observed before in antimony-doped tin oxide samples by Orel et al. [2] for practically the entire range of doping. In addition, the fitting of the thin film diffraction patterns revealed that antimony doping does not influence the cell parameters in spite of the substitution of Sn(IV) by Sb(V) and the new empty sites created in the framework (see Table 1). XPS measurements indicate the existence of some organic compounds not fully pyrolized [4]. Antimony and tin seems to be in an oxygen octahedral environment, as Sb(V) and Sn(IV), respectively.

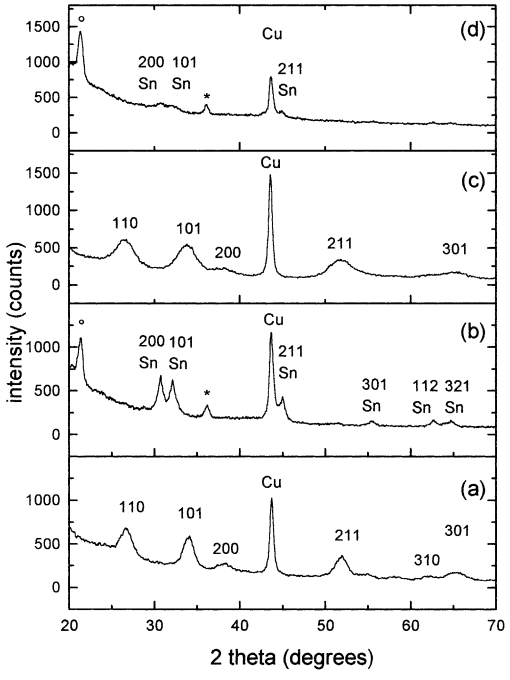

Fig. 1. XRD patterns of tin dioxide-based thin films: (a) not doped, (c) doped with "5% Sb". (b) and (d) difractograms correspond to the films (a) and (b), respectively, after three cycles, in the charge state. °: substrate; *: $Li_{4.4}Sn$.

One important feature is the remarkable increase of the film conductivity when they are antimony-doped (see Table 1). In fact, the values found for the resistivities of antimony-doped films were of the order of a few Ω cm, at least two orders lower than those found for non-doped films. This feature should increase the reactivity of the materials during the first cycle, when tin particles are formed in situ.

Potentiostatic cycles of the thin films were recorded in the voltage range of 50 mV to 1.2 V using 10 mV per 10 min steps. As can be seen in Fig. 2, first discharge profiles are substantially similar to those observed for SnO_2 [5,6], where a strong peak is present in the range 0.9–1.0 V. This peak corresponds to the reaction between tin oxide and lithium leading to the dissociation of the oxide, according to:

$$SnO_2 + 4Li \Rightarrow Sn + 2Li_2O \quad (1)$$

For the antimony-doped samples, the dissociation takes place at higher voltages, in the range 0.9–1.4 V and the peaks are broader than for the non-doped sample. Two reaction schemes can be proposed for the antimony-doped oxides:

tin and antimony formation :

$$Sb_xSn_{1-x}O_2 + Li \Rightarrow (1-x)Sn + xSb + Li_2O \quad (2)$$

tin−antimony alloy formation :

$$Sb_xSn_{1-x}O_2 + Li \Rightarrow Sb_xSn_{1-x} + Li_2O \quad (3)$$

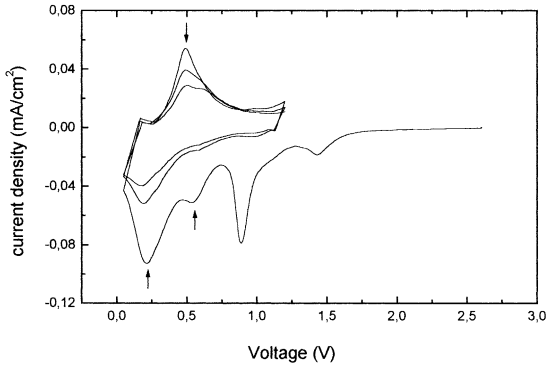

Fig. 2. Potentiostatic cycles for the non-doped tin oxide sample using 10 mV per 10 min steps between 0.05 and 1.2 V.

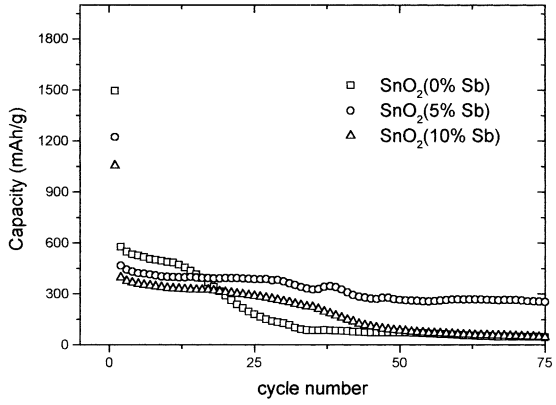

Fig. 3. Capacity (mAh/g) versus cycle number of cells with antimony–tin oxide thin films as anodes.

It is difficult to determine which of these two reactions occurs in the electrode. Nevertheless, the presence of a small peak at approximately 0.85 V, can be associated to the formation of Li_3Sb from antimony–tin alloys [7]. Finally, down to 0.7 V, the reduction peaks agree with the lithium alloying of tin to yield several Li_xSn ($1 \leq x \leq 4.4$) compounds. The lithium extraction from these alloys is indicated in the oxidation profile by the presence of one peak at ca. 0.5 V. The dealloying reaction is not totally reversible according to the areas observed under the reduction and oxidation peaks.

Cells were cycled galvanostatically in a range of 50 mV to 1.2 V under a current density of 0.25 mA/cm^2, corresponding to *C*/7 rates. First discharge capacities are 1495, 1222 and 1054 mAh/g for the "0% Sb", "5% Sb" and "10% Sb" samples, respectively (Fig. 3). Considering the complete tin oxide dissociation, it seems that $Li_{4.4}Sn$, Li_3Sn and Li_2Sn are the limiting alloys for "0% Sb", "5% Sb" and "10% Sb" doping levels. This feature is in good agreement with the reversible capacities found in the first 10 cycles, corresponding practically to their total dealloying. In order to clarify this point, diffraction patterns of the cycled anodes in the charge state were recorded (see Fig. 1b and d). Cassiterite peaks are not present indicating that tin-based dioxides have been totally dissociated. Both tin metal and the $Li_{4.4}Sn$ alloy are detected in all samples. The presence of $Li_{4.4}Sn$, which should no longer exist at 1.2 V, can explain the irreversibility of the electrodic process but contrasts with the expected final composition of the lithium–tin alloy in the doped samples. In these samples, only a certain proportion of tin formed in the first discharge would be electroactive. After 12 cycles, the non-doped sample capacity fades drastically, meanwhile the doped samples retain 300 mAh/g. The "5% Sb" sample shows the best performance, with 250 mAh/g in the 75th cycle. Capacity fading in tin-based systems is due to the impressive cell volume changes associated with the alloying of tin, that leads to a loss of mechanical and electrical contact [1]. This explains the use of very fine tin-based particles, binder and electronic additives for improving the electrode performance. When tin dioxide films are antimony-doped, particles decrease in size and increase their conductivity, suggesting that electrode integrity is maintained more efficiently. In addition, the presence of Sb in the electrode could account for the better cyclability of the antimony-doped samples [3,7] by preventing the growth of large crystallites during cycling.

4. Conclusions

These preliminary results would indicate that Sb doping in SnO_2 thin films significantly enhances the performance of the electrode in a lithium-ion cell. Several reasons can explain this feature. First, the grain size decrease when the tin dioxide film is antimony modified. Second, the thin films must increase their electronic conductivity when doping, thus improving the electrode reactivity during the first cycle. Additionally, antimony doping may limit grain growth during cycling. Further investigation must be carried out in order to clarify the electrode mechanism.

Acknowledgements

The authors would like to thank the EEC for supporting this work through JOULE Contract no. JOR3-CT98-0180, and Mr. Vincent Fernandez (from LPCM, Institute de Matériaux Jean Rouxel, Nantes, France) and Mr. Olivier Crosnier (Ecole Polytechnique de l'Université de Nantes, France) for the XPS measurements.

References

[1] T. Brousse, R. Retoux, U. Hertirich, D.M. Schleich, J. Electrochem. Soc. 145 (1998) 1.
[2] B. Orel, U. Lavrencic-Stangar, K. Kalcher, J. Electrochem. Soc. 141 (1994) L127.
[3] J. Morales, L. Sánchez, J. Electrochem. Soc. 146 (1999) 1640.
[4] R. Ayouchi, F. Martin, J.R. Ramos Barrado, M. Martos, J. Morales, L. Sánchez, J. Power Sources 87 (2000) 106–111.
[5] Y. Idota, T. Kubota, A. Matsufuji, Y. Maekawa, T. Miyasaka, Science 276 (1997) 1395.
[6] I.A. Courtney, J.R. Dahn, J. Electrochem. Soc. 144 (1997) 2045.
[7] J. Yang, M. Winter, J.O. Besenhard, Solid State Ionics 90 (1996) 281.